ATES SMART GRIDS: OPTIMAL USE OF SUBSURFACE SPACE IN HIGH DENSITY ATES AREAS

Martin Bloemendal[1,2]

[1] Delft University of Technology, Stevinweg 1, Delft, Netherlands

[2] KWR Watercycle research institute, Groningenhaven 7 Nieuwegein, Netherlands

j.m.bloemendal@tudelft.nl

Keywords: ATES, heat transport.

ABSTRACT

Aquifer Thermal Energy Storage (ATES) systems provide buildings with sustainable space heating and cooling by seasonally storing and recovering thermal energy in the subsurface. The increased use of ATES in Dutch cities resulted in dense use of ATES in urban aquifers, often up to congestion level. Because thermal interactions among neighbouring systems may improve (same type of wells close together) or degrade (opposite type of wells together) system performance, the spatial layout of ATES wells is a key aspect for this novel energy storage technology. To prevent negative interaction, current policy requires ATES wells to be placed at relatively large distance from each other. However, several studies have shown that wells can be placed closer together, allowing ATES adoption for more buildings than under current policy with the spacious safety margins. Utilising the full storage potential of urban aquifers then requires increasing the density of ATES wells. This density can be further increased using a distributed energy management in which ATES wells can be controlled in order to prevent negative interactions during operation. In this research such a framework was developed. The delivered proof of concept of this framework is carried out by facilitating information exchange between ATES systems and the use of various (types of) model predictive control approaches. Simulated case studies, varying from small academic setting to full size complex urban conditions, have been used to develop and test the framework. Results show a significant decrease of CO_2 emissions by allowing more ATES wells in the urban aquifer. Ongoing research focuses on using this framework in an aquifer beneath a densely populated district of Amsterdam. Results from this case/pilot will be presented.

1. INTRODUCTION

Problem and goal

Aquifer Thermal Energy Storage (ATES) systems provide sustainable heating and cooling for buildings. For sustainable use of ATES, the associated building of an ATES systems needs to have both a heating and cooling demand that are about as large (Bloemendal et al., 2014). Unfortunately, most buildings do not have such a balanced heating and cooling demand profile. Under imbalance conditions solutions exists to obtain extra heat or cooling capacity for individual ATES systems, e.g. via dry coolers from the air of heat exchange in surface water of roads. However, when two nearby buildings have compatible heating and cooling demand profile, it obviously makes sense to transfer the heat surplus of one building to the other with heat shortage. This can either be done via a piped connection or by placing the warm and cold wells of these systems close to each other.

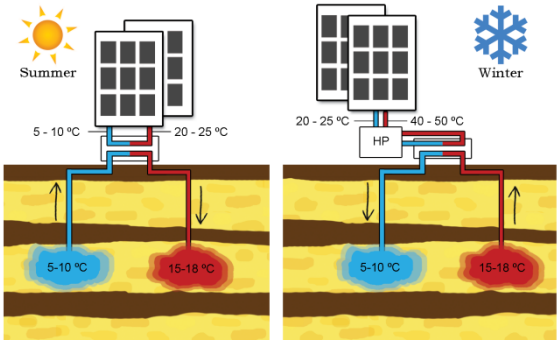

Figure 1. Basic working principle of ATES

At a location in Amsterdam 2 building A & B have a heat surplus, while the nearby building C has a heat shortage[1]. Earlier study (Rijswijk and Oosten, 2018) showed that making a piped connection is too expensive due to a busy street in between the building A & B and the building C. Therefore, it is also not possible to place the warm and cold wells of the system close to each other. But on the other hand, the street is not very wide and since the aquifer that is used for heat storage is continuous under the street, it may be possible to transport the heat through the aquifer from one to the other side of the street.

The goal of this study is to explore under which conditions it is possible and efficient to use the aquifer

[1] For privacy reasons the ATES system owners have been anonymized.

for heat transport from the buildings A & B to the building C.

Approach

First the energy demand profiles are identified in order to obtain how much heat needs to be transported. two scenarios are considered, 1) current ATES use of buildings A&B and 2) future ATES use. (Currently the Buildings also use boilers and chillers for a considerable part their heating and cooling demand. However, at some point these have to be replaced by more heat pump and ATES capacity.)

Secondly the subsurface conditions are identified together with possible well locations.

As a final step the information from the first two steps is brought together in a geohydrological model, which is then used to evaluate the rate of heat transfer from one side of the street to the other. Depending on the results and possible well locations various scenarios will be evaluated to explore under which conditions subsurface heat transport is possible and efficient.

2. METHODS & MATERIALS

Energy demand of the buildings

The energy demand and ATES use of the buildings has been identified by Rijswijk and van Oosten (Rijswijk and Oosten, 2018). The building C does not have an ATES system currently, but for this approach to be successful they need to install an ATES. For the use of ATES it is assumed that 100% of the cooling demand is supplied from the cold well and 100% of the heating demand by a heat pump with a COP of 5, from which the heat required from the ATES can be calculated (Bloemendal et al., 2018). Assuming a temperature difference between the warm and cold well of 6° C together with a volumetric heat capacity of water (c_w) of 4.2 x 10^6 [J/m^3/C] can then be used to identify the required groundwater for each well, Table 1**Error! Reference source not found.**.

Table 1. Heating and cooling from wells (Rijswijk and Oosten, 2018)

System	Heating *[MWh]*	Cooling *[MWh]*	+/- *[MWh]*
A Current	400	600	200
Future	1,280	1,600	320
B Current	1,000	1,400	400
Future	1,840	4,000	2,160
C Current	960	400	-560
Future	960	400	-560

In the "current" situation the heat surplus of the buildings A&B already match the heat shortage of building C. So in the future situation there is also an amount of about 2,000 MWh of heat available for other buildings. For the future analysis it is assumed that the ATES of the building B will be connected to the nearby hotels or houses, these details are not included/elaborated. It is simply assumed that the building C will take up any heat surplus of buildings A&B. This is mainly to assess whether the efficiency/ feasibility of the concept of subsurface heat transport is sensitive to scale at which heat needs to be transported.

Subsurface conditions and well characteristics

The subsurface of Amsterdam consists of a 60m thick covering layer, mainly made up of clay and peat, Figure 2. From 60m depth and onwards a thick aquifer exists until a depth of about 220m depth. This thick aquifer is utilized for ATES. The well screens of the A & B building ATES system are also in this aquifer, Table 2.

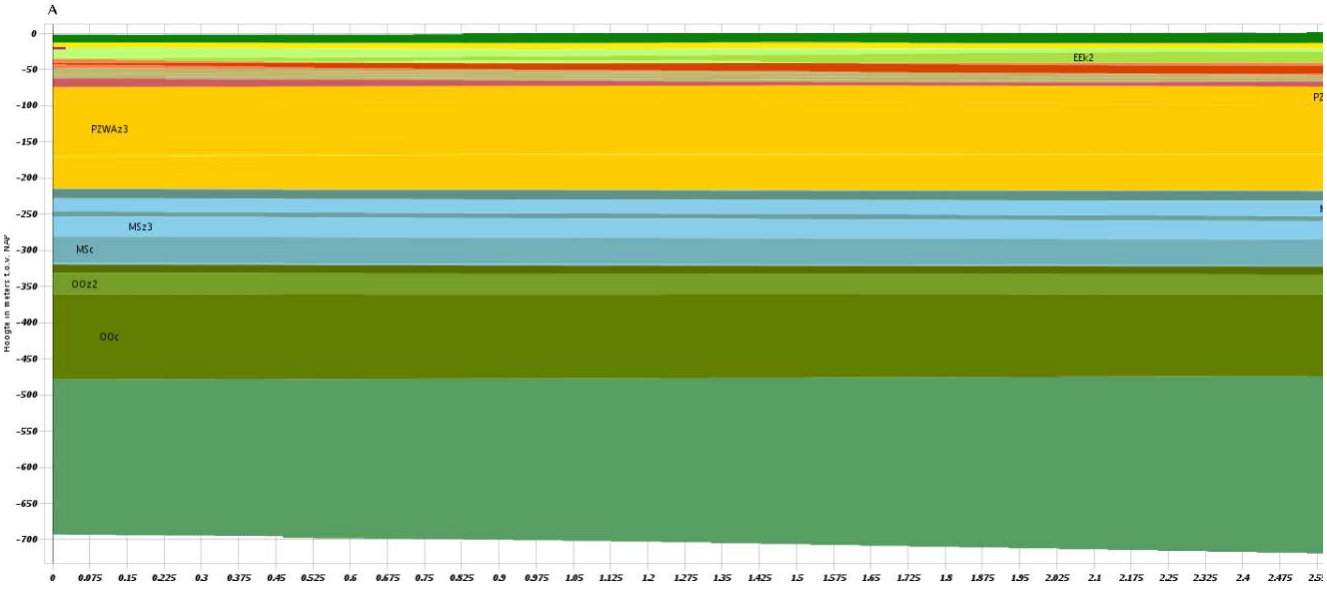

Figure 2. Subsurface model of Amsterdam according to REGIS (TNO, 2002). Yellow layers from 60-220 m are sandy layers from the Peize-Waalre formation, targeted for ATES.

Building A has a monowell system, while building B has a doublet. For the exploratory simulations, only the wells of building B will be used, assuming the heat surplus of building A can be diverted into the warm well of the building B. The warm and cold well of the building C will be placed in at the building C side of the street. Depending of the results of the simulation the wells may be placed closer to the street if needed. Especially the cold well of the building B is far away from the street, and may be needed to be moved closer to achieve subsurface heat transport. The minimum distance that can be realized is about 30m (from side walk to side walk crossing the street), so that is also the minimum distance that is used in the simulations. For the future scenarios the distance between warm and cold wells also needs to be larger, so cold wells may also be moved south of the nearby crossroads, resulting in a maximum distance between warm and cold wells of about 140m.

The screens of the wells of building B are 110m according to database of local authority. This seems relatively long, and it is not clear if this is the actual installed screen length. Shorter screen lengths, cause larger lateral spreading of the heat, so to promote heat transport also scenarios with shorter screens are simulated.

Table 2. well properties, [meter –surface level]

System	Well type	Warm screen *top-bottom*	Cold screen *top-bottom*
A	Monowell	77-95	113-131
B	Doublet	91-200	91-200

Assessment framework

The thermal energy stored in an ATES system can have a positive and negative temperature difference between the infiltrated water and the surrounding ambient groundwater, for either heating or cooling purposes. In this study the thermal energy stored is referred to as heat or thermal energy; however, all the results discussed equally apply to storage of cold water used for cooling. Like in other ATES studies (Doughty et al., 1982; Sommer, 2015), the recovery efficiency (η_{th}) of an ATES well is defined as the amount of injected thermal energy that is recovered after the injected volume has been extracted. For this ratio between extracted and infiltrated thermal energy (E_{out}/E_{in}), the total infiltrated and extracted thermal energy is calculated as the cumulated product of the infiltrated and extracted volume with the difference of infiltration and extraction temperatures ($\Delta T = T_{in} - T_{out}$) for a given time horizon (which is usually one or multiple storage cycles), as described by:

$$\eta_i\left(t_0 \rightarrow t\right) = \frac{E_{out,i}}{E_{in,i}} = \frac{\int_{t_0}^{t} \Delta T_{out,i} Q_{out,i} dt}{\int_{t_0}^{t} \Delta T_{in,i} Q_{in,i} dt} = \frac{\Delta \overline{T}_{out,i} V_{out,i}}{\Delta \overline{T}_{in,i} V_{in,i}} \quad [1]$$

with, Q being the well discharge during time step t and $\Delta\overline{T}$ the weighted average temperature difference between extraction and injection. Injected thermal energy that is lost beyond the volume to be extracted, is considered lost as it will not be recovered. To allow unambiguous comparison of the results the simulations in this study are carried out with constant yearly storage and extraction volumes, but please note that due to the required transport, $V_{in} \neq V_{out}$ for individual wells. This will then have a large influence on the recovery efficiency of each wells, the warm well of the building C will extract more then it will infiltrate and thus have a higher efficiency.

Next to the recovery efficiency also the weighted average extraction temperature is an important measure for how successful the heat transport is.

Losses due to mechanical dispersion and conduction occur at the boundary of the stored body of thermal energy, the thermal recovery efficiency therefore depends on the geometric shape of the thermal volume in the aquifer (Bloemendal and Hartog, 2018; Doughty et al., 1982). Following Doughty, the infiltrated volume is simplified as a cylinder with a thermal radius (R_{th}) defined as:

$$\mathrm{R}_{th} = \sqrt{\frac{c_w V}{c_{aq} \pi L}} \quad [2]$$

The size of the thermal cylinder thus depends on the storage volume (V), screen length (L, for a fully screened aquifer), porosity (n) and water and aquifer heat capacity (c_w, c_{aq}). This equation is approximate because heterogeneities and partially penetration of the screens are ignored.

Simulation tools

As losses due to conduction, dispersion and displacement occur simultaneously, MODFLOW (Harbaugh et al., 2000) is used to evaluate their combined effect on recovery efficiency. For the simulation of groundwater flow and heat transport under various ATES conditions, a geohydrological MODFLOW model coupled to the transport code MT3DMS (Hecht-Mendez et al., 2010; Zheng and Wang, 1999) is used. These model codes use finite differences methods to solve the groundwater and (heat) transport equations. This allows for simulation of infiltration and extraction of groundwater in and from groundwater wells and groundwater temperature distribution, as was done in previous ATES studies e.g. (Bloemendal et al., 2018; Bonte, 2013; Caljé, 2010). In the different modelling scenarios the storage volume is varied between 57,000 and 600,000 m^3 according to the required storage capacities introduced in Table 1, with flow rates proportionally ranging. Density differences are neglected as this is considered a valid assumption (Caljé, 2010; Doughty et al., 1982) for the considered ATES systems that operate within a limited temperature range (<25°C). The parameter

values of the model are given in Table 3, the following discretization was used:

- Model layers; the storage aquifer is confined by two clay layers, following the composition in Figure 2. The storage aquifer is divided in 10m thick model layers, the middle layers' thickness is changed according to the required screen length of the modeled scenario.
- The spatial discretization used in horizontal direction is 5 x 5 m at well location, gradually increasing to 250 x 250 m at the borders of the model. A sufficiently large model domain size of 6x6 km was used to prevent boundary conditions affecting (<1%) simulation results. The gradually increasing cell size with distance from the wells results the cell size of 15 m at 200 m of the well. This discretization is well within the minimum level of detail to model the temperature field around ATES wells as was identified by Sommer (Sommer et al., 2015). The street and well locations are oriented diagonally in the field. To allow for straight forward visualisation of temperature profiles in the aquifer, the well locations are oriented in x-y direction in the simulation grid. The mutual distances between the wells correspond to the distances that are present or can be realized in practice.
- A temporal discretization of one week is used, which is sufficiently small to take account for the seasonal operation pattern and resulting in a courant number smaller than 0.5 within the area around the wells where the process we care about occur. The simulation has a horizon of 10 years, sufficiently long to achieve stabilized yearly recovery efficiencies.

The PCG2 package is used for solving the groundwater flow, and the MOC for the advection package simulating the heat with a courant number of 1. To set the desired ambient groundwater flow velocity for the different scenarios simulated, the constant hydraulic head boundaries were used to set the required hydraulic gradient. In the aquifer an ATES doublet is placed with a well distance of five times the maximum thermal radius of the wells to avoid mutual interaction between the warm and cold storage volumes. In scenarios with groundwater flow, the ATES wells are oriented perpendicular to the flow direction.

The energy demand profile of ATES systems varies due to variations in weather conditions and building use. The yearly storage volumes are distributed over the simulation period following a cosine function.

3.RESULTS

Current ATES use

For each simulation scenario, the recovery efficiency and average extraction temperature are indicated in Table 4. Topview and cross section temperature distributions in the aquifer are used to discuss the simulation results

Table 3, MODFLOW simulation parameter values (Caljé, 2010; Hecht-Mendez et al., 2010)

Parameter	value
Horizontal conductivity aquifers	25 m/d
Horizontal conductivity aquitards	0.05 m/d
Longitudinal dispersion	1 m
Transversal dispersion	0,1 m
Bulk density	1890 kg/m^3
Bulk thermal diffusivity	0.16 m^2/day
Solid heat capacity	880 J/kg °C
Thermal conductivity of aquifer	2.55 W/m °C
Effective molecular diffusion	$1 \cdot 10^{-10}$ m^2/day
Thermal distribution coefficient	$2 \cdot 10^{-4}$ m^3/kg
Injection temperature cold / warm wells	5 / 15 °C

BASE CASE. In the base case simulation the warm wells are at about 50m distance and the cold wells at about 120m. The distance between the cold and warm well of the building C is about 85m. Figure 3 shows that after 5 years the cold wells do not form one single cold well and also that there is some interaction between the warm and cold wells. Figure 5 shows a cross section of the temperature distribution in the aquifer at the last summer and winter of the 5 year simulation period. This also indicates that the warm wells may be placed closer together to obtain more efficient heat transport. with the screen lengths and storage volumes of the base scenario, the Thermal radii of the individual wells vary between 15 and 35m, indicating that at 50m distance they only touch, resulting in less efficient heat transport.

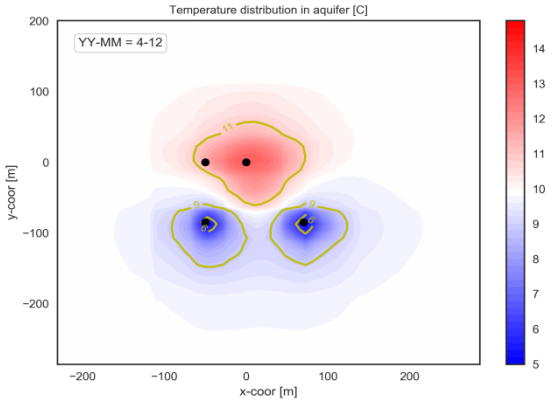

Figure 3. Simulation results of base scenario in last winter of the 5 year simulation period. The yellow contours indicate the 6, 9, 11 and 14 °C thresholds

CLOSER. By placing the wells more optimal the performance of the heat transport increases. Well distance is now set to 30m for same type of wells and to 100m between warm and cold wells. Figure 6 shows that there are now combined warm and cold wells, also the 6 and 14 ° C contours are no longer separated. Also the efficiencies and extraction temperatures improve.

SHORTER SCREENS. Following the design rules introduced by Doughty et al. and Bloemendal and Hartog (Bloemendal and Hartog, 2018; Doughty et al., 1982) the optimal screen length for the required storage temperatures varies between 40 to 65m. So for this scenario the screen length is set to 50m for all wells, resulting in thermal radii between 25 and 50m. The locations are 50m separated (base case for warm wells). Results (Table 4, Figure 7 top) indicate that shortening the screens indeed improves the working conditions, although not as much as when placing the wells closer together.

SHORTER SCREENS & CLOSER. In this scenario wells of the same type are separated again at 30m, the distance between cold and warm wells is 140m. These conditions give the best result.

Table 4, Simulation results, last years efficiency and last years average extraction temperature for current ATES use scenarios

Well: building:	**Cold C** η T	**Warm C** η T	**Cold A&B** η T	**Warm A&B** η T
Base	0.19 7.7	0.73 11.5	0.50 8.2	0.41 12.8
Closer	0.21 7.5	1.02 12.1	0.63 7.7	0.40 12.7
shorter screens	0.22 7.3	0.86 11.7	0.57 7.9	0.41 12.7
screens & closer	0.22 7.3	1.09 12.2	0.66 7.6	0.41 12.8

Please note that:

A) The warm well of the building C and the cold well of building B has a larger extraction than infiltration volume, the efficiency is therefore higher, and vice versa for the cold well of the building C and warm well of building B. Heat transport works the best when the average extraction temperature is highest for the warm well of the building C and lowest for the cold well of building B.

B) When simulating only building B, the last years recovery efficiency and extraction temperatures of the warm and cold well are 0.48/12.3 and 0.44/7.7 respectively. The large well screens relative to the storage volume cause these poor efficiencies. Placing wells of the building C (or any other building) will already improve performance as can be seen from the base case results.

Future energy demand for ATES

For each simulation scenario, the recovery efficiency and average extraction temperature are indicated in Table 5. Topview and cross section temperature distributions in the aquifer are used to discuss the simulation results

BASE. In the base case simulation the warm wells are at about 50m distance and the cold wells at about 120m. The distance between the cold and warm well of the building C is about 85m. Figure 4 shows that after 5 years the cold wells do not form one single cold well and also that there is some interaction between the warm and cold wells. For the cold wells it is still needed to place the wells closed together, for the warm wells it may still help but not as much in the current ATES use scenario in the previous section. With the screen lengths and storage volumes of the future scenario, the thermal radii of the individual wells vary between 15 and 60m, indicating that at 50m distance they already overlap, resulting in more efficient heat transport. Also the small distance between warm and cold wells negatively influences the efficiency.

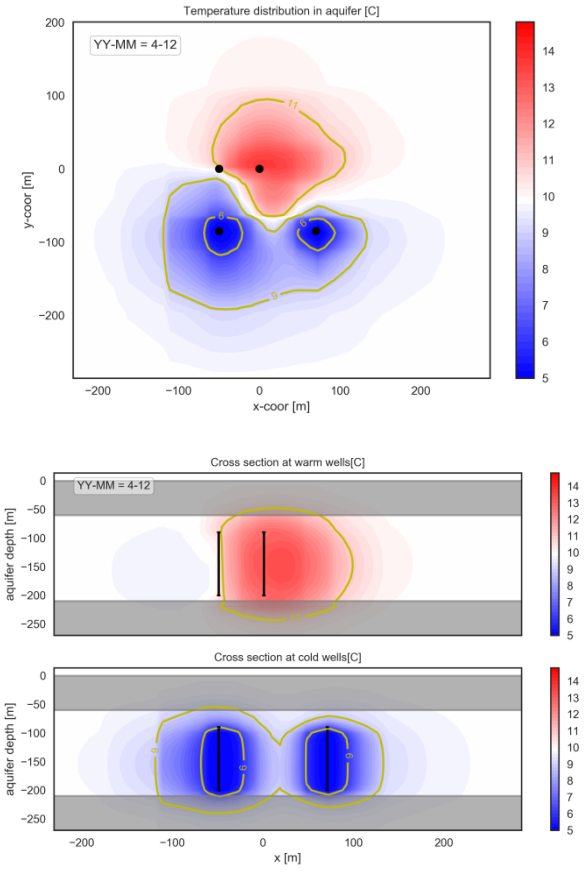

Figure 4. Simulation results of future scenario in last winter of 5 year simulation period. The yellow contours indicate the 6, 9, 11 and 14 °C thresholds

CLOSER. By placing the wells more optimal the performance of the heat transport increases. Well distance is now set to 30m for the cold wells and to 140m between warm and cold wells. Figure 8 shows that there are now combined warm and cold wells, also the 6 and 14 °C contours are no longer separated. Also the efficiencies and extraction temperatures improve.

SHORTER SCREENS & CLOSER. Following the design rules introduced by Doughty et al. and Bloemendal and Hartog (Bloemendal and Hartog, 2018; Doughty et al., 1982) the optimal screen length for the required storage temperatures varies between 70 to 95m. So for this scenario the screen length is set to 80m for all wells, resulting in thermal radii between 20 and 70m. The locations are 30m separated. Results (Table 5, Figure 9) indicate that shortening the screens does not improve the working conditions, which can be explained by flattening of the optimum screen length at larger storage volume (Bloemendal and Hartog, 2018).

Table 5, Simulation results, last years efficiency and last years average extraction temperature for future ATES use scenarios

Well: building:	**Cold C** η T	**Warm C** η T	**Cold A&B** η T	**Warm A&B** η T
Base	0.10 6.3	1.28 10.9	0.51 8.5	0.39 13.3
Closer	0.09 6.7	2.68 11.8	0.89 7.4	0.40 13.4
screens & closer	0.09 6.7	3.26 12.2	0.89 7.4	0.37 13.2

4. DISCUSSION AND CONCLUSIONS

Short term perspective

With current set-up of warm and cold well locations of building B is hard to accomplish effective heat transport. For the warm well it is possible, although a smaller distance and/or shorter screen is preferable. However, for the cold wells, no combined cold zone will be formed (also not after 25 years of simulation, which was also simulated but not presented). So in the case the buildings A&B can operate with a relatively high extraction temperature from the cold well, and the province would issue a permit for such large cold well, only adding wells for building C is needed.

However, preferably the cold well of the A&B buildings are moved to the street and also the warm well of building B is moved 20m closer to the street, to create combined warm and cold wells.

Next steps

- It is important to be confident on the actual installed screen length of the well of building B. When the screen is indeed 110m, identify if it is possible to apply a packer halfway the screen to shorten it.
- Identify if it is possible / cost effective to connect ATES well of building A to warm well of the building B.
- Identify if it is possible / cost effective it place the wells of the building C in the side walk of the busy street.
- Economic evaluation of required system changes at buildings A&B side, and installation at building C side.

Long term perspective

With larger storage volumes, heat transport is easier to achieve. However, as a result of increasing thermal radii, mutual interaction between wells also occurs.

next steps

- Explore the possibility to separate warm and cold wells even further than currently identified maximum of 140m along the streer.
- Simulation is carried out with single wells, in practice most likely mutiple doublets may be required. Identify the need for additional doublets and explore the possibility to improve transport by control of infiltration/extraction rates of wells
- Identify if there is additional heat demand for the large heat surplus of buildings A&B.

General conclusions and next steps

This case study indicated that subsurface heat transport has potential under specific conditions. Only site specific conditions where addressed in this research. Next ongoing steps are to further assess applicability under a wider range of geohydrological and ATES conditions.

Acknowledgements

This research was supported by the Netherlands Organization for Scientific Research (NWO) and the Amsterdam institute for metropolitan solutions (AMS) as part of the Uncertainty Reduction in Smart Energy Systems (URSES+) research program, under the project Aquifer Thermal Energy Storage Smart Grids (ATES-SG), grant number 408-13-030.

REFERENCES

- Bloemendal, M., Hartog, N., 2018. Analysis of the impact of storage conditions on the thermal recovery efficiency of low-temperature ATES systems. Geothermics 17, 306-319.
- Bloemendal, M., Jaxa-Rozen, M., Olsthoorn, T., 2018. Methods for planning of ATES systems. Applied Energy 216, 534-557.
- Bloemendal, M., Olsthoorn, T., Boons, F., 2014. How to achieve optimal and sustainable use of the subsurface for Aquifer Thermal Energy Storage. Energy Policy 66, 104-114.

- Bonte, M., 2013. Impacts of shallow geothermal energy on groundwater quality, geo sciences. Vrije Universiteit Amsterdam, Amsterdam.
- Caljé, R., 2010. Future use of aquifer thermal energy storage inbelow the historic centre of Amsterdam, Hydrology. Delft University of Technology, Delft.
- Doughty, C., Hellstrom, G., Tsang, C.F., 1982. A dimensionless approach to the Thermal behaviour of an Aquifer Thermal Energy Storage System. Water Resources Research 18, 571-587.
- Harbaugh, A.W., Banta, E.R., Hill, M.C., McDonald, M.G., 2000. Modflow-2000, the u.S. Geological survey modular ground-water model—user guide to modularization concepts and the ground-water flow process in: USGS (Ed.). US Geological Survey, Virginia.
- Hecht-Mendez, J., Molina-Giraldo, N., Blum, P., Bayer, P., 2010. Evaluating MT3DMS for Heat Transport Simulation of Closed Geothermal Systems. Ground water 48, 741-756.
- Rijswijk, R., Oosten, B.v., 2018. Verdiepingsonderzoek museumplein zuidereiland. Merosch.
- Sommer, W., 2015. Modelling and monitoring Aquifer Thermal Energy Storage. Wageningen University, Wageningen.
- Sommer, W., Valstar, J., Leusbrock, I., Grotenhuis, T., Rijnaarts, H., 2015. Optimization and spatial pattern of large-scale aquifer thermal energy storage. Applied Energy 137, 322-337.
- TNO, 2002. REGIS, Utrecht.
- Zheng, C., Wang, P.P., 1999. MT3DMS: A Modular Three-Dimensional Multispecies Transport Model for Simulation of Advection, Dispersion, and Chemical Reactions of Contaminants in Groundwater Systems; Documentation and User's Guide.

FIGURES

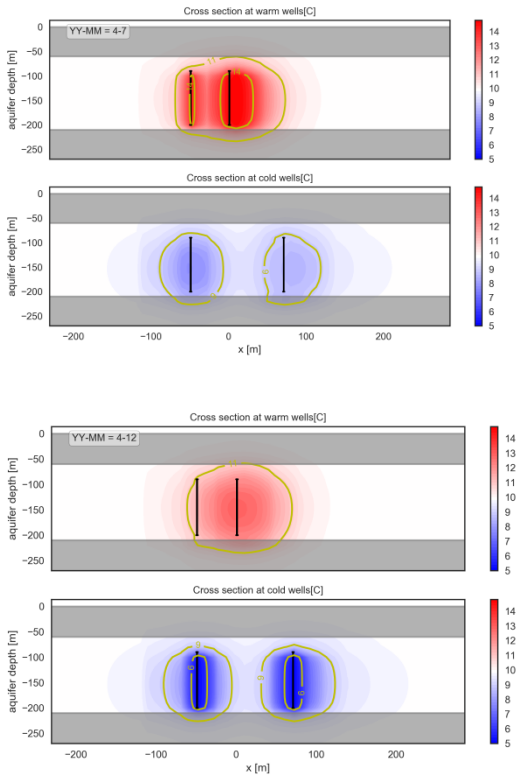

Figure 5. Simulation results of base scenario in last summer (top) and last winter (bottom) of 5 year simulation period. The yellow contours indicate the 6, 9, 11 and 14 °C thresholds

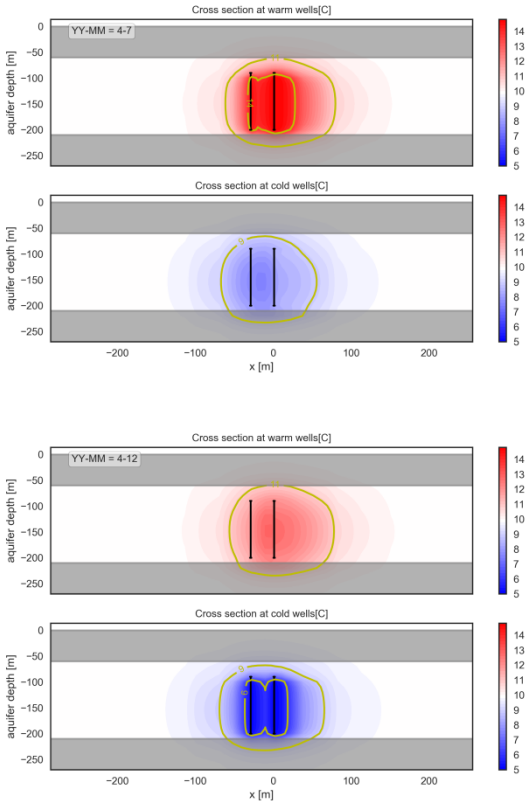

Figure 6. Simulation results of optimal well location scenario for current ATES use in last summer (top) and last winter (bottom) of 5 year simulation period. The yellow contours indicate the 6, 9, 11 and 14 °C thresholds

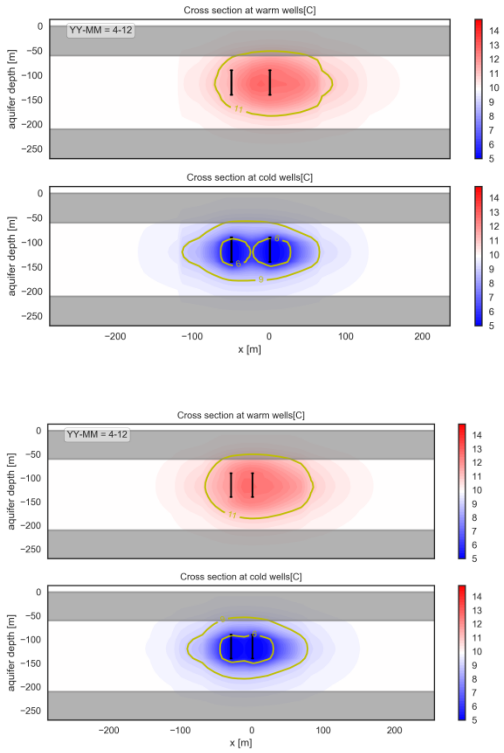

Figure 7. Simulation results in the last winter (bottom) of 5 year simulation period of the shorter screen (top) and more optimal well location (bottom) scenarios for current ATES use. The yellow contours indicate the 6, 9, 11 and 14 °C thresholds

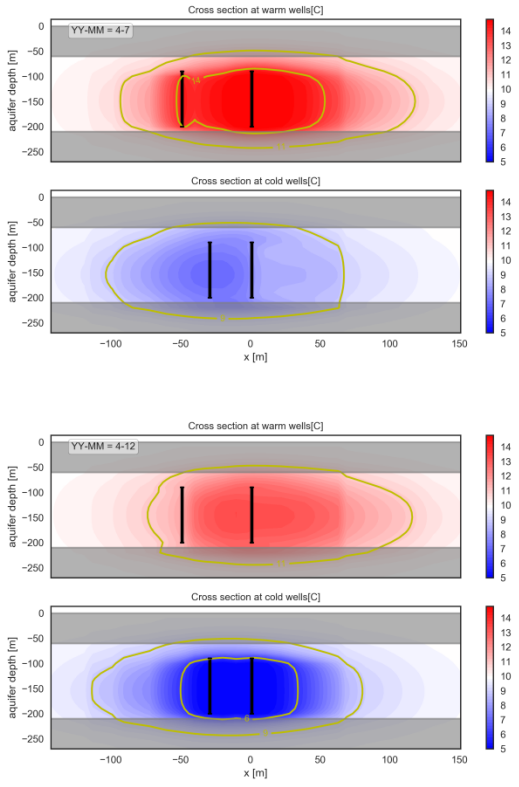

Figure 8. Simulation results of optimal well location scenario for future ATES use in last summer (top) and last winter (bottom) of 5 year simulation period. The yellow contours indicate the 6, 9, 11 and 14 °C thresholds

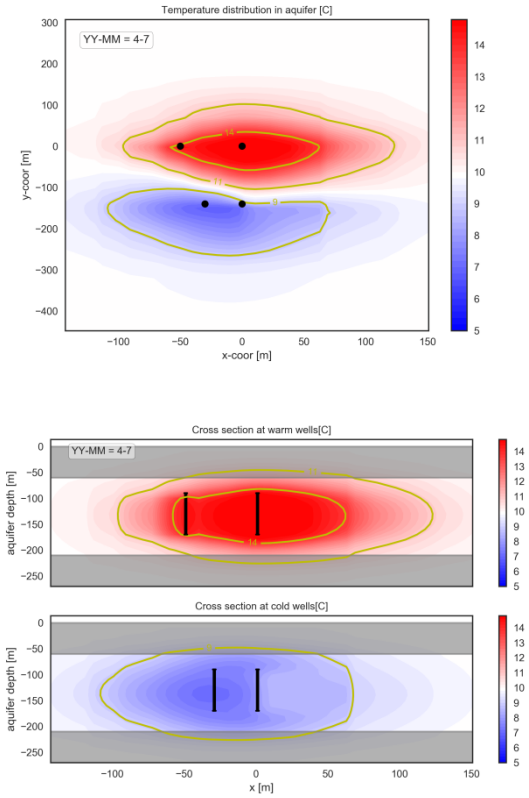

Figure 9. Simulation results in the last summer of 5 year simulation period of the shorter screen and more optimal well location scenarios for future ATES use. The yellow contours indicate the 6, 9, 11 and 14 °C thresholds